



Article

Tribological Behavior of Ti-Coated Diamond/Copper Composite Coating Fabricated via Supersonic Laser Deposition

Qunli Zhang^{1,2,3} , Yiyun Chen^{1,2,3}, Bo Li^{1,2,3}, Changyi Wang^{1,2,3}, Lijuan Wu^{1,2,3} and Jianhua Yao^{1,2,3,*}

¹ Institute of Laser Advanced Manufacturing, Zhejiang University of Technology, No. 288 Liuhe Road, Hangzhou 310023, China

² College of Mechanical Engineering, Zhejiang University of Technology, No. 288 Liuhe Road, Hangzhou 310023, China

³ Key Laboratory of Special Purpose Equipment and Advanced Processing Technology, Ministry of Education and Zhejiang Province, Zhejiang University of Technology, No. 288 Liuhe Road, Hangzhou 310023, China

* Correspondence: laser@zjut.edu.cn

Abstract: Diamond/copper composite coating is promising for wear-resistant applications, owing to the extreme hardness of the diamond reinforcement. Ti-coated diamond/copper composite coatings with various laser powers were successfully fabricated employing the novel manufacturing technology of supersonic laser deposition (SLD). Ti-coated diamond, which was able to enhance the wettability between diamond and copper, was prepared at the optimal parameters via salt bath. Nano-spherical titanium carbides were uniformly distributed on the diamond's surface to generate a favorable interface bonding with a copper matrix through mechanical interlocking and metallurgical bonding during impact. Furthermore, the results showed that the transition layer acted as a buffer, preventing the breakage of the diamond in the coating. SLD can prevent the graphitization of the diamonds in the coating due to its low processing temperature. The coordination of laser and diamond metallization significantly improved the tribological properties of the diamond/copper composite coatings with the SLD technique. The microhardness of the diamond/copper composite coating at a laser power of 1000 W reached about 172.58 HV_{0.1}, which was clearly harder than that of the cold sprayed copper. The wear test illustrated that the diamond/copper composite coating at a laser power of 1000 W exhibited a low friction coefficient of 0.44 and a minimal wear rate of 11.85 μm³·N⁻¹·mm⁻¹. SLD technology shows great potential in the field of preparing wear-resistant hard reinforced phase composite coatings.

Keywords: supersonic laser deposition; Ti-coated diamond; diamond/copper composite coating; wear-resistant



Citation: Zhang, Q.; Chen, Y.; Li, B.; Wang, C.; Wu, L.; Yao, J. Tribological Behavior of Ti-Coated Diamond/Copper Composite Coating Fabricated via Supersonic Laser Deposition. *Lubricants* **2023**, *11*, 216. <https://doi.org/10.3390/lubricants11050216>

Received: 14 April 2023

Revised: 5 May 2023

Accepted: 10 May 2023

Published: 11 May 2023



Copyright: © 2023 by the authors. Licensee MDPI, Basel, Switzerland. This article is an open access article distributed under the terms and conditions of the Creative Commons Attribution (CC BY) license (<https://creativecommons.org/licenses/by/4.0/>).

1. Introduction

Copper and its alloys have been widely employed in the sectors of power electronics, energy, machinery, and transportation owing to its easy processing, corrosion-resistant, and electrical and thermal conductivity properties [1,2]. Due to their notoriously inferior wear resistance, copper components always undergo severe wear and erosion during daily service, which significantly shortens their service life [3]. On the contrary, the inherent ultra-hardness, large bulk modulus, and outstanding tribological properties of diamond enables it to be a superior wear-resistant material [4]. However, industrially produced diamond has limited crystal size and is challenging to machine due to its intrinsic properties. Therefore, understanding how to make full use of the advantages of diamond in industrial production has become a hot research topic.

The increased mechanical performances of diamond/copper composite indicate the remarkable improvements of the composite, which can acquire the benefits of both diamond and copper [5,6]. The ductility of the copper matrix provides the machinability of the composite, while the diamond-reinforced phase improves the wear resistance of the

composite [7]. However, the poor wettability between diamond and copper causes the composite interface to have obvious defects, which seriously affect the performance of the composite [8]. Therefore, the diamond will spall in friction wear due to poor bonding. To overcome the drawback of poor interfacial bonding, construction of transition layers by chemical reactions use elements such as B [9], Cr [10], Ti [11], and W [12] to enhance the bonding between the reinforcing phase and the matrix through the wettability between carbide and copper. Carbide transition layers can effectively avoid diamond flaking in frictional wear and thus take full advantage of diamond wear resistance.

Currently, diamond/copper composites are mainly produced through powder metallurgy and metal infiltration. Powder metallurgy usually fabricates composites via pressurized sintering of copper and diamond mixed powder, such as spark plasma sintering [13], vacuum hot pressing [14], and high-temperature high-pressure process [15]. The sintering temperature of powder metallurgy is below the melting point of copper, which means that the diamond and copper powder is still linked in the form of particles with poor interface bonding. Moreover, the diamond floats during the sintering process due to its relatively low density, which leads to the uneven distribution of the two phases in the composite. On the contrary, the infiltration method [16–18] is employed to fabricate composites by melting copper at a high temperature and then infiltrating it into the preforms of diamond under pressure or no pressure conditions. The principle is mainly to cause the molten copper to enter the interstices between the diamonds using the capillary effect. The drawbacks are that the diamond is prone to ablation at temperatures of over 1000 °C, the need to provide an oxygen-free atmosphere to safeguard the composite from oxidation, and the high temperature and pressure leading to huge costs. In order to prepare diamond/copper composites with superior properties, there is an urgent need to develop a high-quality and efficient manufacturing technology that avoids the drawbacks of existing technologies.

Supersonic laser deposition (SLD) is a promising addition to manufacturing and surface modification technology [19]. During the spraying process, micron-sized powder is accelerated to 300–1400 m/s using high pressure gas through a de-Laval nozzle under laser irradiation and achieves deposition via severe plastic deformation through kinetic energy and heat energy [20]. Metals [21,22], composites [23], and even ceramics [24] have been successfully fabricated via SLD with favorable performance. SLD is dominated by kinetic energy and supplemented by thermal energy, which avoids oxidation defects, thermal residual stress, and thermal damage caused by the high-temperature preparation of composites. Furthermore, SLD can be applied to rapidly prepare various structures, coatings on any surface, and efficiently repair damaged parts [25]. As a brittle and hard material, diamond has a high critical deposition rate in commercial cold spraying, which is prone to internal fracture and cannot be effectively plastically deformed to achieve deposition. By constructing a buffer layer on the surface of diamond and introducing laser thermal softening via SLD, diamond composites can be deposited. Previous studies have rarely focused on the manufacturing and the wear resistance of core-shell diamond/copper composite coatings.

In this paper, diamond is coated with Ti via salt bath to bridge the large gap of acoustic impedance and enhance the bonding between the diamond and copper. The novel SLD additive manufacturing process is applied to prepare machinable Ti-coated diamond/copper composite with excellent wear-resistant performance. The composition, microstructure, and tribological characteristics of the diamond/copper composite coatings were thoroughly investigated after preparation at various laser power. The purpose of this paper is to improve the wettability between diamond and copper by diamond surface modification, while introducing laser to enhance interfacial bonding. It ensures that the diamond can play an excellent wear resistance role in the diamond/copper composite coating without flaking.

2. Materials and Methods

2.1. Composite Fabrication

The feedstock for SLD included irregular copper powder (Zhongke Yanuo Technology Co., Ltd., Beijing, China) ranging from 15 to 53 μm in size and irregular diamond powder (Zhongyuan Superhard Co., Ltd., Tuocheng, Henan, China) ranging from 35 to 42 μm in size after commercially available spherical Ti ranging from 15 to 48 μm in size plating via salt bath. Figure 1 shows the morphology of the original powder. Ti-coated diamonds are prepared using the salt bath method at 900 $^{\circ}\text{C}$ for 1 h to build a uniform density of carbide transition layer.

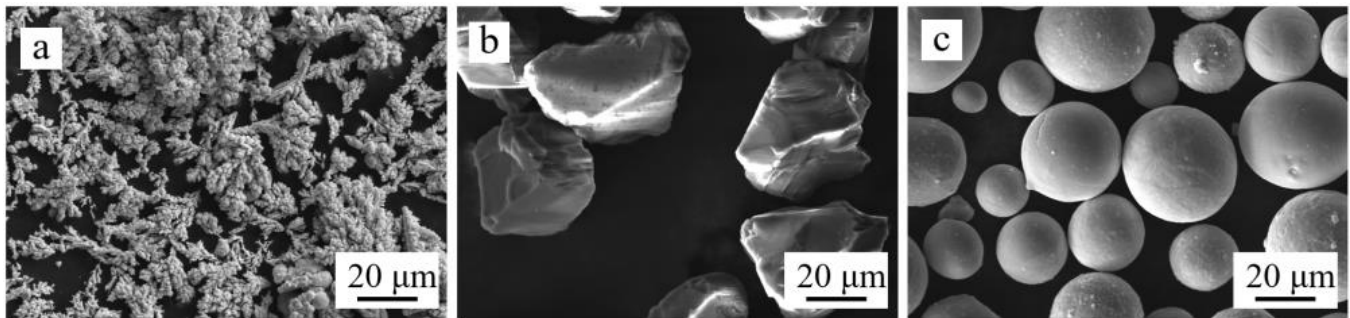


Figure 1. Morphology of the (a) copper, (b) diamond, and (c) Ti used in this study.

The Ti-coated diamond/copper composite coatings were fabricated onto the copper substrate using an in-house SLD system. The system was mainly composed of a six-axis mechanical arm, powder feeder, high pressure nitrogen station, water cooling system, gas heating device, and laser system (LDF6000-100 VGP, Laserline, Koblenz, Germany) [7]. The schematic of the fabrication via SLD is shown in Figure 2. The spraying nozzle had a total length of 278.0 mm with a throat diameter of 2.8 mm and an exit diameter of 6.0 mm. The produced coatings and SLD parameters are presented in Table 1. The copper and 50 vol% Ti-coated diamond powder were mechanically mixed before spraying. Through previous preparatory experiments, we observed that the composite coating suffered from poor interfacial bonding at a laser power of about 500 W, while the interfacial bonding was favorable at 1000 W. Too high a laser power leads to problems of diamond graphitization and local thermal stress concentration. Therefore, 0 W, 500 W, 1000 W, 1500 W were chosen as experimental parameters to study the effect of laser power and its different effects on the composite coatings. For facilitating the following discussion, each composite coating was marked using an abbreviation. The abbreviation ‘C’ means the as-deposited composite coating, while ‘0’, ‘500’, ‘1000’, and ‘1500’ indicate the laser power used to produce the composite coating. The laser and the spray gun were fixed on the mechanical arm and moved with the same traversal speed. All composite coatings were prepared at a stand-off distance of 30.0 mm and 3.0 MPa nitrogen pressure with a traversal speed of 10 $\text{mm}\cdot\text{s}^{-1}$. The speed of the powder feeder was set to 2 RPM. The diamond particles were estimated 435–563 $\text{m}\cdot\text{s}^{-1}$ at a powder-heating temperature of 500 $^{\circ}\text{C}$ [20]. The Ti-coated diamond/copper composite coatings were fabricated onto the sand-blasted copper substrate using 24 μm corundum.

Table 1. Abbreviations of the prepared coatings and the SLD conditions.

Annotation	Laser Power [W]	Temperature [$^{\circ}\text{C}$]
C ₀	0	500
C ₅₀₀	500	500
C ₁₀₀₀	1000	500
C ₁₅₀₀	1500	500

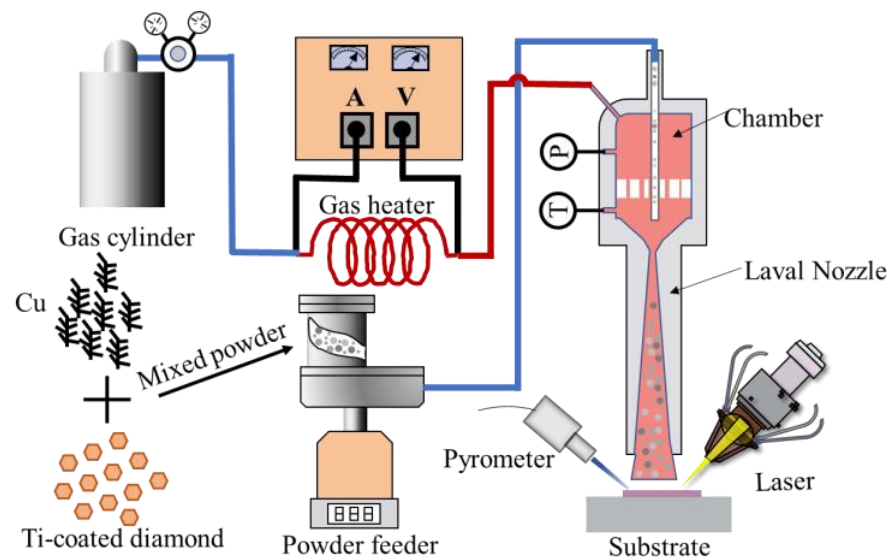


Figure 2. Schematic of the fabrication of the Ti-coated diamond/copper composite coatings via SLD.

2.2. Material Characterizations

The X-ray diffractometer (D8 Advance, Bruker, Billerica, MA, USA) was employed to investigate the phase composition of the samples using SLD with the copper ($\lambda = 1.542 \text{ \AA}$) source at a current of 40 mA, a voltage of 40 kV, and scan step of 0.02° . In order to prevent the metallographic procedure from damaging the morphology of the diamond in the coating, the fracture morphology of the coating was investigated. Scanning electron microscopy (SEM, EVO 18, Carl Zeiss, Stuttgart, Germany) was employed to analyze the morphology of the samples, and the elemental composition was determined using affiliated energy-dispersive spectroscopy (EDS, Nano X-flash Detector 5010, Bruker).

2.3. Wear Test

The Vickers hardness tester (HMV-2, SHIMADZU, Kyoto, Japan) was used to test the microhardness of the samples with a load of 0.98 N for 15 s. A small amount of ultra-high hardness was caused by the indentation on the diamond. The hardness of the samples was determined by averaging 10 hardness values in order to be accurate. A ball-on-disc tribometer (HT-600, Lanzhou Institute of Chemical Physics, Lanzhou, China) was employed to measure the tribological properties of the samples at room temperature. The samples were polished with a 2.5 \mu m metallographic polishing agent before the test to ensure the accuracy of the wear test. A silicon nitride ball with a diameter of 5 mm was used as a counter-grinding part to contact the fixed sample on the disc. The disk rotated at a speed of $350 \text{ r}\cdot\text{min}^{-1}$ under a load of 5N. The wear mechanism was investigated using SEM, EDS, and LSCM. The wear rate was obtained by calculating the volume of wear per unit length under unit load. The mean COF (μ), wear radius (r), and wear cross-sectional area (S) of each specimen was measured. The wear volume (V) was calculated as follows:

$$V = 2 \cdot \pi \cdot r \cdot S \quad (1)$$

3. Results and Discussion

3.1. Composition and Morphology of Metallized Diamond

Figure 3 exhibits the surface morphology of the diamond after Ti plating via salt bath. Compared with the original diamond in Figure 1b, it is obvious that almost all the diamonds were coated with a shell as seen in Figure 3a. The surface of the shells with significantly improved roughness was undulating and had a granular bulge, which contributed to the subsequent SLD coating preparation. In order to better observe the effect of metallized diamond via salt bath, the edge of an uncoated diamond is shown in Figure 3b. It was

observed that the thickness of the transition layer closely combined with diamond was only 2–3 μm , which was thinner than the 6 μm copper-nickel layer of the diamond [26]. This was mainly due to the chemical reaction between Ti and carbon on the surface of the diamond to generate chemical bonding, which would protect the diamond and improve the wettability with copper in coating preparation using SLD. The titanium element reacted with the diamond in the molten salt through the following equations [7]:

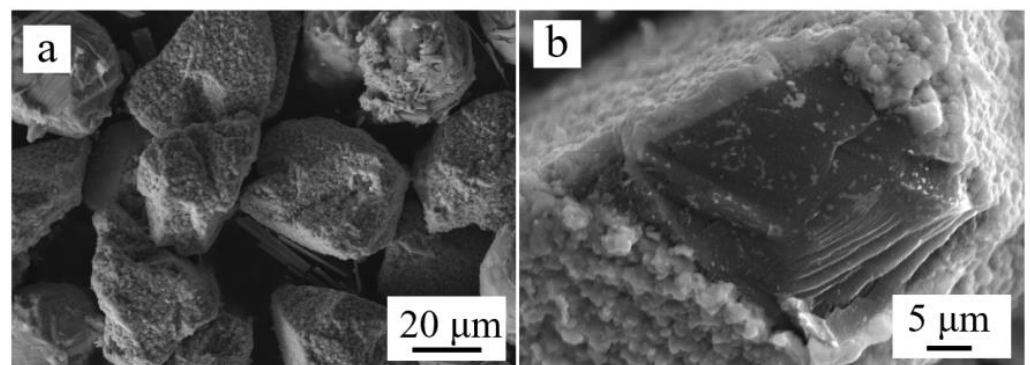
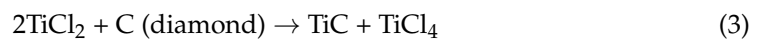


Figure 3. SEM images of (a) the Ti-coated diamond powder and (b) the cross-section of typical Ti-coated diamond.

The molten salt provided a flow atmosphere at a high temperature, which caused the diamond surface to react completely.

The XRD diffractions of diamond before and after salt bath plating are shown in Figure 4. Although the diamonds were almost completely coated as shown in Figure 3, the diamond's characteristic peaks were still detected from the diffraction of the Ti-coated diamond, so it can be concluded that the layer was thin. The characteristic peaks of TiC indicate that TiC successfully coated the surface of the diamond [27]. The characteristic peaks of Ti clearly showed that metal titanium also existed on the diamond's surface. The many miscellaneous peaks were mostly different types of titanium carbide, indicating that the transition layer presented gradient carbide changes.

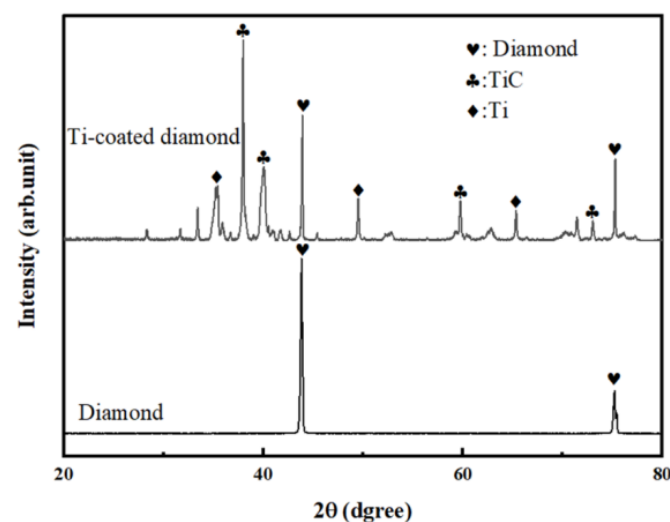


Figure 4. XRD profiles of the diamond powder before and after Ti coating.

3.2. Composites Prepared via SLD with Different Laser Power

The XRD spectra of Ti-coated diamond/copper composite coatings at various laser powers are depicted in Figure 5. Due to the relatively small content of diamond, the characteristic peaks of copper were mainly detected. When the laser power was high, the diamond deposition efficiency was improved, as can be seen in the dashed frame, which confirmed the positive effect of laser power. A small number of the characteristic peaks of diamond and titanium carbide were observed. No graphite peaks appeared at 26.5° , indicating that the diamond phase in the composite maintained its original properties with SLD [28].

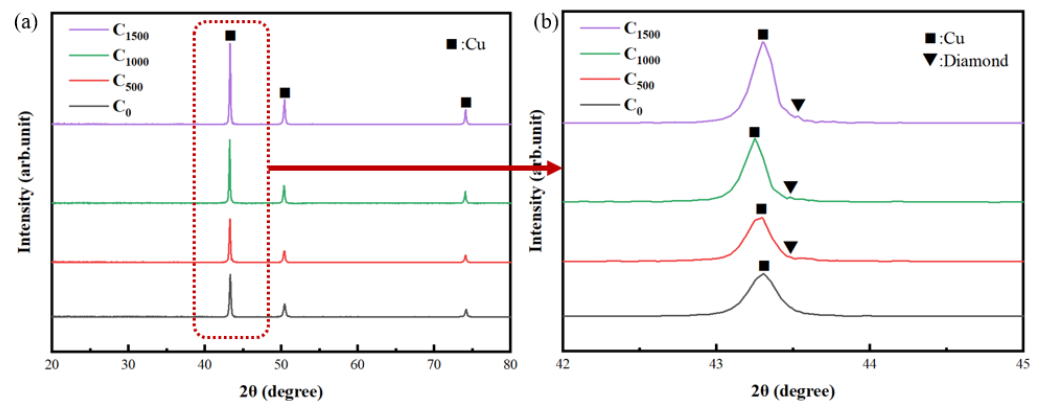


Figure 5. XRD patterns (a) and their partially enlarged detail (b) of the Ti-coated diamond/copper composites at various laser power.

The SEM images of the fracture cross-section of the Ti-coated diamond/copper composite coatings fabricated via SLD at various laser powers are shown in Figure 6. The deposition efficiency of diamond was significantly improved as the laser power increased. The pits left by the diamond shedding after the fracture were formed due to poor interface bonding under cold spraying without laser irradiation, as can be seen in Figure 6a. However, it was observed that the transition layer on the surface of the diamond peeled off in Figure 6b, which was due to the breakage of the transition layer during impact at a low laser power. As the laser power reached 1000 W, the diamond with high deposition efficiency retained most of the transition layer to protect the brittle diamonds. This was due to the better particle softening and copper plastic deformation capability of the laser and the resultant lower particle critical impact velocity. Due to the softening effect of laser irradiation on particles, the phenomenon of diamond breakage or rebound was reduced, and the deposition efficiency was improved [20]. As the laser power reached 1500 W, excessive thermal stress leads to a large number of tiny pores at the particle interface during cooling, which affected the performance of the composite coating.

The magnified SEM images of Ti-coated diamond/copper composite coatings at various laser powers are exhibited in Figure 7. As seen in Figure 7a, without the laser irradiation, the cracks in the diamond and the pores at the edge were obvious in the coating, which lead to the spalling of the diamond. At the laser power of 500 W, as shown in Figure 7b, a small number of cracks could still be seen in the coating, but the interfacial bonding was greatly improved compared to the coating without laser addition. When the laser power was 1000 W, the cracks at the interface no longer appeared (as in Figure 7c) due to the softening of the interface using laser energy. The shell of the Ti-coated diamond was deformed during the impact process, which reduced the brittle fracture of the diamond and may have produced the interpenetration of interface elements due to its wettability with the copper matrix. However, when the plastic flow of the copper matrix was large with a high laser power (in Figure 7d), the mutual impact between diamonds resulted in cracks during the deposition process.

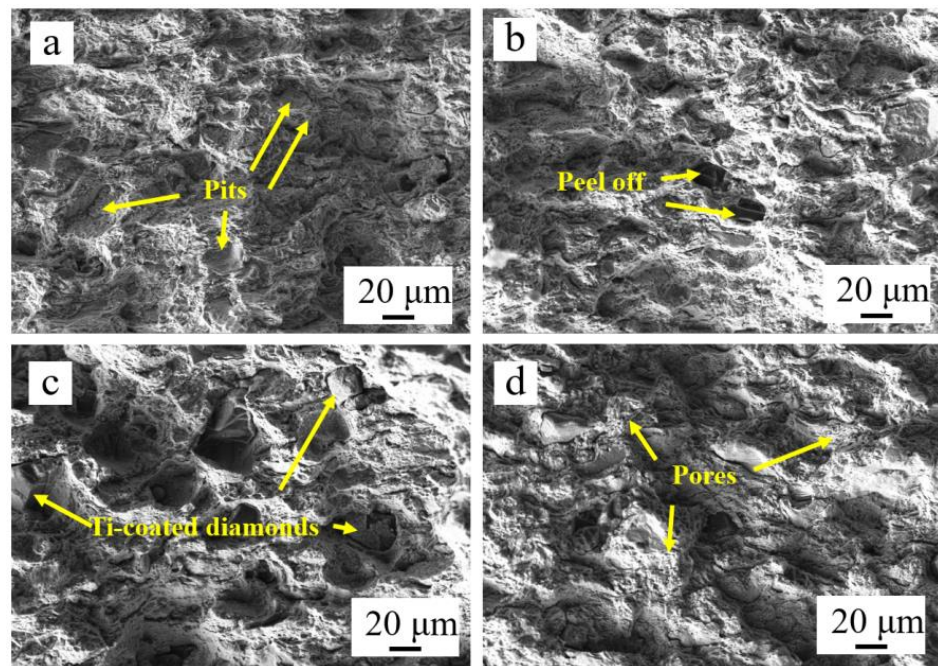


Figure 6. SEM images of the Ti-coated diamond/copper composite coatings at various laser power: (a)— C_0 , (b)— C_{500} , (c)— C_{1000} , (d)— C_{1500} .

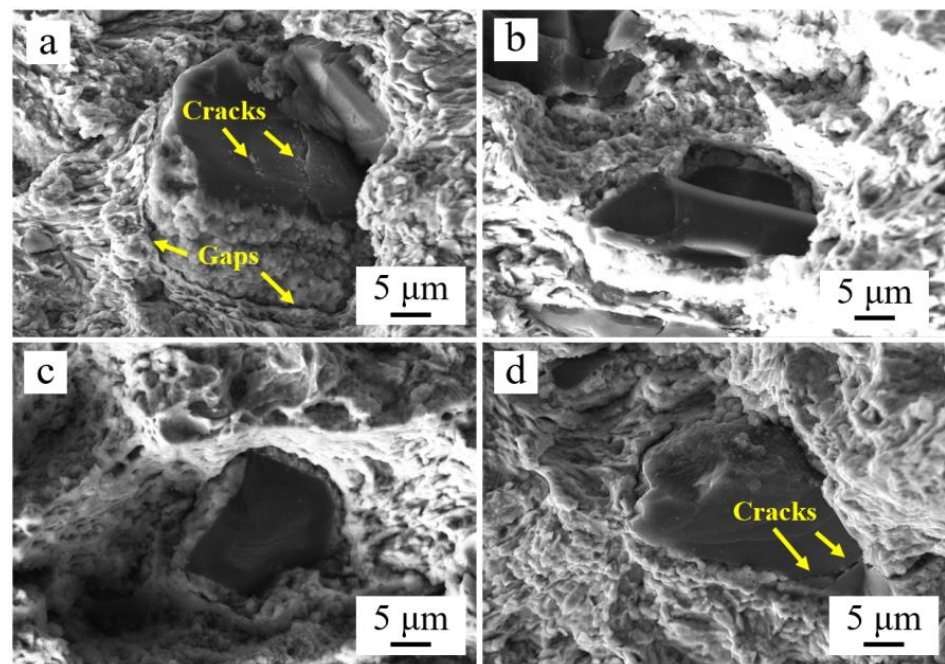


Figure 7. The magnified SEM images of the Ti-coated diamond/copper composite coatings at various laser powers: (a)— C_0 , (b)— C_{500} , (c)— C_{1000} , (d)— C_{1500} .

To study the element distribution at the interface between diamond and copper, the typical characteristics of Ti-coated diamond in C_{1000} is analyzed in Figure 8. The titanium element around the diamond can be clearly observed, which was connected to the copper element. A line scan at the interface showed a 0.5 μm overlap between copper and titanium, and a 0.8 μm overlap between titanium and carbon. The transition layer of the diamond was infiltrated with copper elements under the action of the laser, which proved the excellent combination of diamond in the composite. In the SLD process, the deposition mechanism of core-shell diamond particles was mainly a cushioning protection mechanism for the shell

structure under the high speed impact. Without laser irradiation, the cracks on the surface of the diamond and the broken transition layer can be seen in Figure 7a after deposition. The sample prepared at a lower laser power due to work hardening was not able to avoid the peeling of the titanium carbide or even the fracture of the diamond. However, too high a laser power resulted in the same appearance due to the impact between diamonds. The high-speed impact diamond particles were deposited by the buffer of the transition layer to protect the diamond. Additionally, the transition layer and the copper element penetrated each other to achieve an effective combination at an optimal laser power.

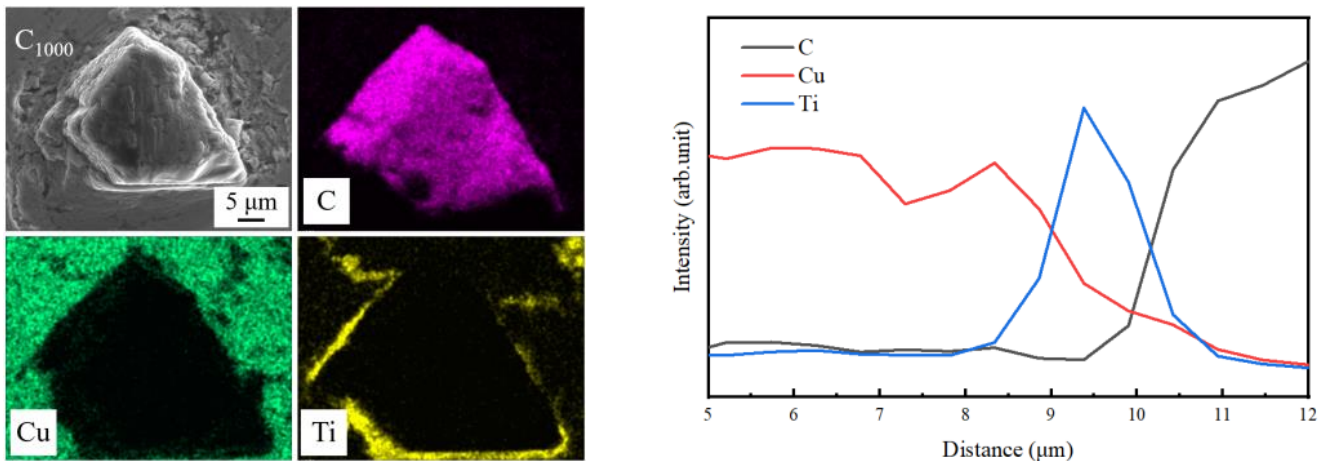


Figure 8. EDS mapping and line scanning at the interface of the Ti-coated diamond for C₁₀₀₀.

3.3. Wear-Resistant Property

The microhardness of the Ti-coated diamond/copper composite coatings at various laser powers is shown in Figure 9. The substrate hardness of the composite was 93 HV_{0.1}. Clearly, the microhardness of all the laser-irradiated samples was harder than that of the cold sprayed copper due to the hammer effect of the diamond and the softening effect of laser irradiation [29]. In addition, although the diamond content in the composites enhanced with the increase of laser power, the hardness increased first and then decreased. Laser irradiation played different roles at various laser powers—with a low laser power, the microhardness was mainly caused by the hammer effect of the diamond and the work hardening caused by the plastic deformation of the copper. The maximal hardness reached 172.58 ± 4.05 HV_{0.1} at 500 W. Laser irradiation may have caused tempering, resulting in a reduction of hardness [30]. As the laser power increased, the composite material was tempered and the grains at the interface were re-crystallized, which refined the grains and lead to the release of residual stresses, thus reducing the hardness. The diamond content no longer played a major role, and the microhardness decreased to 128.70 ± 8.72 HV_{0.1} at 1500 W.

Figure 10 displays the friction curves of C₀, C₅₀₀, C₁₀₀₀, and C₁₅₀₀ at the load of 5 N for 60 min. The average friction coefficients of C₀, C₅₀₀, C₁₀₀₀, and C₁₅₀₀ were 0.65, 0.49, 0.44, and 0.39, respectively. The friction coefficients of all samples rose swiftly in the early stage of sliding friction and became stable with small fluctuations after 5 min, except for C₀. C₀ abruptly fluctuated up and down for 10 min, owing to the friction instability caused by the peeling of the diamond in the composite without the laser. C₀ had the highest friction coefficient due to the poorly bonded particles with small plastic deformation, which lead to abrasive wear. The friction coefficients of C₅₀₀, C₁₀₀₀, and C₁₅₀₀ decreased with the increase of laser power. Due to the thermal stress concentration in the local area at 1500 W laser power, the stress released in friction lead to microcracks, which enhanced the lubrication effect of the copper in the unit contact area.

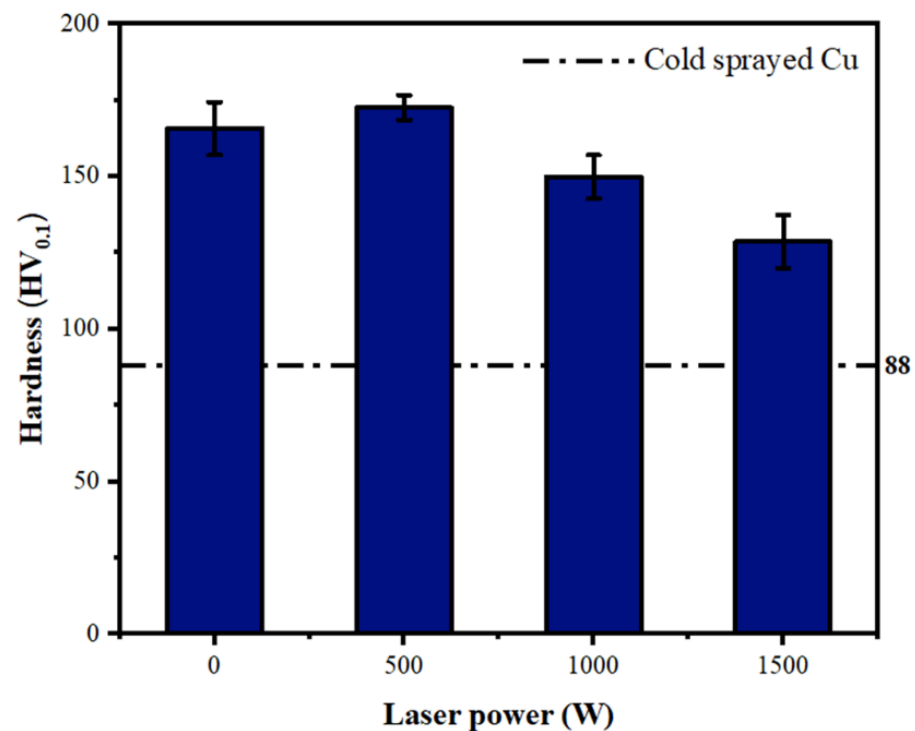


Figure 9. Microhardness of Ti-coated diamond/copper composite coatings at various laser powers.

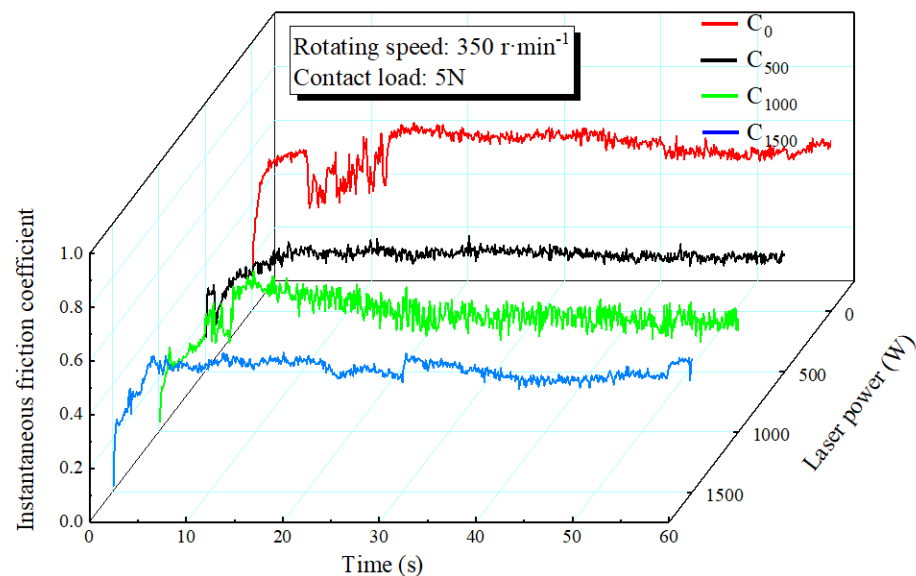


Figure 10. Evolution of the instantaneous friction coefficient at various laser powers.

An LSCM examination was conducted on the surface of the samples to evaluate surface wear. As shown in Figure 11, the roughness change of the worn track in the radial direction are illustrated. The surface roughness of C₅₀₀ (Ra: 9.935 μm), C₁₀₀₀ (Ra: 6.438 μm), and C₁₅₀₀ (Ra: 8.403 μm) was smaller than that of C₀ (Ra: 16.770 μm). By comparing the roughness, the C₁₀₀₀ exhibited a smoother worn surface than that of the others, with a maximum between peak and valley of 12.875 μm . The wear rates of the diamond/copper composite coatings after the wear experiment are shown Table 2. The C₁₀₀₀ composite coating with a wear rate of 11.85 $\mu\text{m}^3 \cdot \text{N}^{-1} \cdot \text{mm}^{-1}$ exhibited better wear resistance performance than that of the C₀, C₅₀₀, and C₁₅₀₀ due to their much higher diamond content.

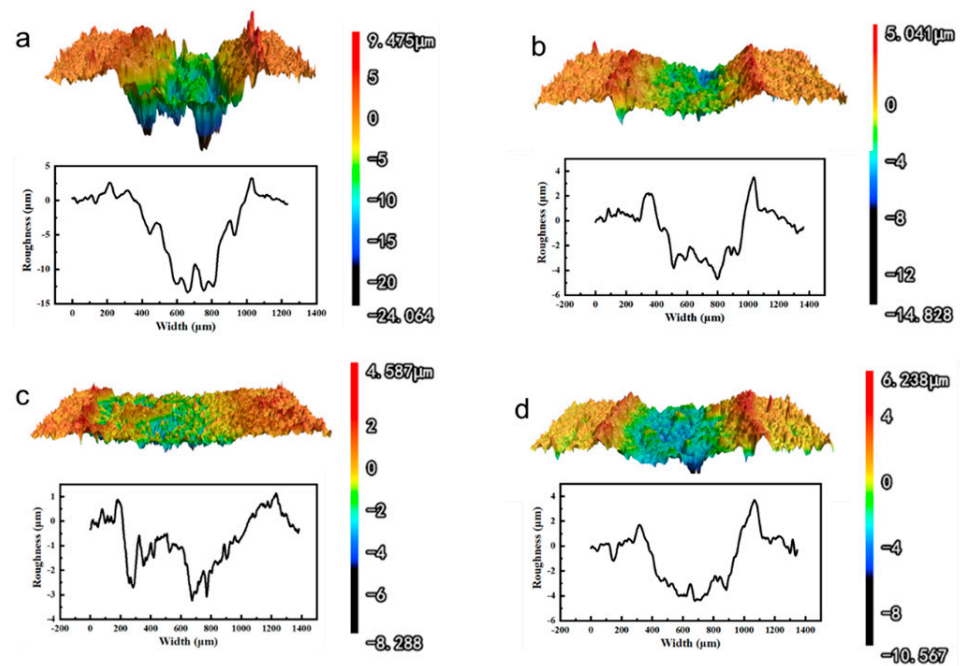


Figure 11. LSCM images of the composite coatings after the ball-on-disk test: (a)— C_0 , (b)— C_{500} , (c)— C_{1000} , (d)— C_{1500} .

Table 2. Wear rates ($\mu\text{m}^3 \cdot \text{N}^{-1} \cdot \text{mm}^{-1}$) of the composite coatings after the ball-on-disk test.

Sample	C_0	C_{500}	C_{1000}	C_{1500}
Wear rate	44.59	14.81	11.85	15.89

In the wear experiment, the diamond in the coating was continuously compacted with time under the action of load. The wear mechanism of the diamond/copper composites was studied by observing the surface of the samples after the wear experiments, shown in Figure 12. The uniformly distributed diamond particles were observed in the four samples after the wear test, indicating that the diamond/copper composite prepared using SLD had promising wear resistance potential. With the increase in wear time, the diamond was embedded in the copper matrix under the protection of the transition layer, which had excellent interface bonding, and thus protected the wear of the composite coating. Due to the low hardness of the copper matrix, the copper gradually adhered to the periphery of the diamond under the action of the hard grinding part with the increase in wear time. Due to the lack of a laser, the poor interface bonding of particles of C_0 resulted in large spalling during friction, as seen in Figure 12a. After the introduction of the laser, the surface peeling of C_{500} was reduced, but it still did not fully play the role of a diamond. As shown in Figure 12c, due to the high content of diamond in C_{1000} , the interaction of diamond particles in wear lead to partial spalling and aggregation under the action of the grinding part. Some pits and grooves appeared in the worn surface. The wear track of C_{1000} showed island adhesion and spalling with a high diamond content, which possessed the best friction and wear properties. Further increasing the laser power led to a downtrend in the hardness of the coating, which resulted in large-scale adhesive wear, as seen in Figure 12d. The lamellar structure was prone to flaking, resulting in a high wear rate.

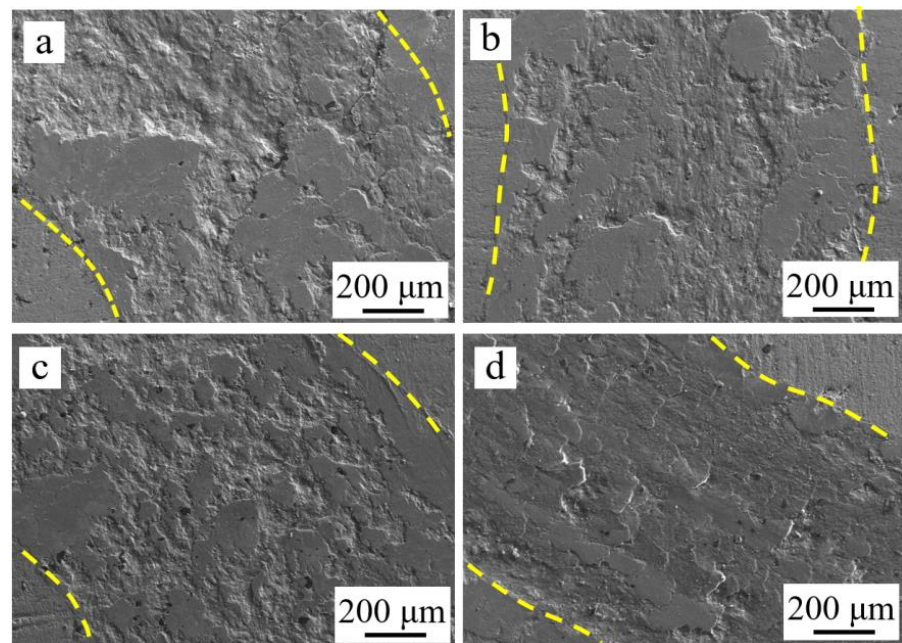


Figure 12. SEM images of the composite coatings after the ball-on-disk test: (a)—C₀, (b)—C₅₀₀, (c)—C₁₀₀₀, (d)—C₁₅₀₀.

The element distribution on the surface after wear was analyzed by observing C₁₀₀₀ with EDS energy spectrum, as shown in Figure 13. The main elements of the worn surface were Cu, O, and C. As the sliding proceeded, the copper chips converged in the local area, while the other part of the copper was oxidized at a high temperature after forming adhesive wear. As the wear time increased, the oxide layer appeared to begin fatigue spalling. The diamond was still evenly distributed throughout the matrix. The presence of the diamond provided a wear-resistant frame for the composite coating, which provided an effective obstacle to the matrix during the wear process and prevented the rapid wear of the matrix.

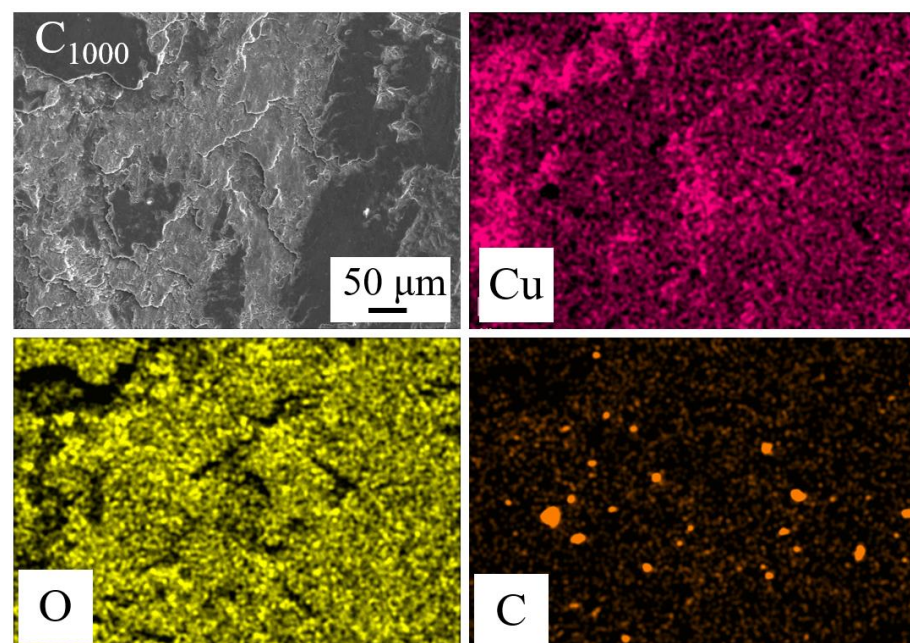


Figure 13. EDS mapping of the composite coating for C₁₀₀₀ after the ball-on-disk test.

The wear mechanisms of the diamond/copper composites prepared via SLD mainly included adhesion, oxidation, and ploughing [31]. The relatively low hardness and high ductility of the copper matrix caused the coating to be mainly adhesive wear. During the sliding process, the rough surface in the initial stage caused the copper matrix to wear continuously. As the diamond began to play a role, it protected the copper matrix from continuous wear and formed plough wear. With the increase in time, the area outside the furrow formed an oxidation lubrication grinding at a high temperature. From Figure 12c, it is evident that a large amount of diamond hindered the plastic deformation of the copper. The element of the transition layer of the Ti-coated diamond and the copper element continuously infiltrated each other during cyclic wear, as shown in Figure 14. Under the hindrance of the diamond, the copper chips were observed to be ground into nano-scale, which helped to improve the wear resistance of the composite coating [32]. The transition layer on the surface of the diamond was worn, but the diamond was still tightly embedded in the matrix and tightly bonded. The element distribution diagram also revealed that the diamond had a strong combination with the copper matrix through the metallized transition layer after friction and the wear test.

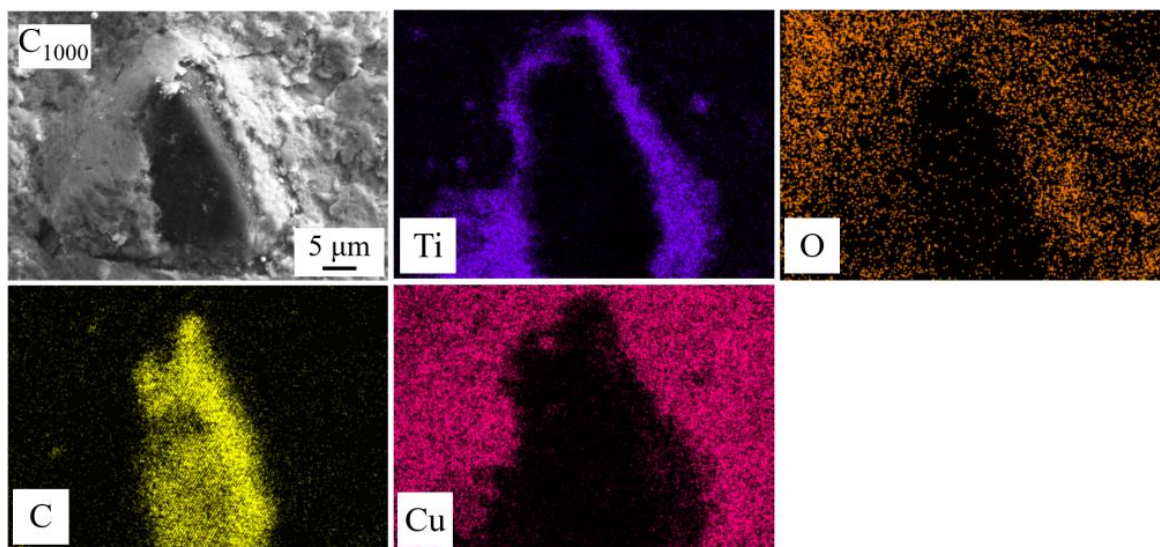


Figure 14. EDS mapping of Ti-coated diamond for C₁₀₀₀ after wear.

4. Conclusions

In summary, Ti-coated diamond/copper composite coatings were fabricated employing solid-state SLD technology using metallized diamond and copper composite powder as feedstock. The SLD technology used a high energy laser beam to heat the deposited powder and substrate simultaneously during the cold spray process. It softened the powder and the matrix, improving the plastic deformation ability and promoting the deposition efficiency, compactness, and interfacial bonding strength of the coating. Through experimental characterization and analysis, we drew the following conclusions:

- (1) The Ti-coated diamond improved the bonding with the copper matrix and played an important role in friction and wear, showing great potential as feedstock for SLD.
- (2) The synergistic effect of laser irradiation and diamond metallization was able to improve the interfacial bonding to ensure that the diamond did not peel off. The interfacial bonding of the Ti-coated diamond/copper composite coating prepared at a laser power of 1000 W was the best without cracks at the interface.
- (3) The Ti-coated diamond/copper composite coatings fabricated using SLD had superior wear-resistant properties, and the coating with higher diamond content had better wear resistance. The microhardness of the Ti-coated diamond/copper composite

- coating at a laser power of 1000 W reached about 172.58 HV_{0.1}, which exhibited the lowest friction coefficient of 0.44 and the minimal wear rate of 11.85 μm³·N⁻¹·mm⁻¹.
- (4) The adhesive wear and oxidation wear were the main wear mechanisms with a small amount of ploughing wear. The oxidation of the copper provided lubrication and improved the wear resistance property.

Author Contributions: Methodology, B.L.; Formal analysis, C.W. and L.W.; Writing—original draft, Y.C.; Writing—review & editing, Q.Z. and J.Y. All authors have read and agreed to the published version of the manuscript.

Funding: This project is support by the National Natural Science Foundation of China (52075495), the Zhejiang Provincial Natural Science Foundation (LY22E050017), and the Science and Technology Project of State Grid Ningxia Electric Power Co., Ltd. (5229CG200069).

Data Availability Statement: No new data were created or analyzed in this study. Data sharing is not applicable to this article.

Conflicts of Interest: The authors declare no conflict of interest. The authors declare that this study received funding from the National Natural Science Foundation of China (52075495), the Zhejiang Provincial Natural Science Foundation (LY22E050017), and the Science and Technology Project of State Grid Ningxia Electric Power Co., Ltd. (5229CG200069). The funders were not involved in the study design, collection, analysis, interpretation of data, the writing of this article, or the decision to submit it for publication.

References

1. Zuo, J.; Lin, Y. An investigation of thermal-mechanical interaction effect on PVD coated tool wear for milling Be/Cu alloy. *Vacuum* **2019**, *167*, 271–279. [[CrossRef](#)]
2. Shaik, M.A.; Golla, B.R. Development of highly wear resistant Cu–Al alloys processed via powder metallurgy. *Tribol. Int.* **2019**, *136*, 127–139. [[CrossRef](#)]
3. Kumar, L.; Singh, H. Effect of nanostructured Cu on microstructure, microhardness and wear behavior of Cu-xGnP composites developed using mechanical alloying. *J. Compos. Mater.* **2021**, *55*, 2237–2248. [[CrossRef](#)]
4. Erdemir, A.; Martin, J.M. Superior wear resistance of diamond and DLC coatings. *Curr. Opin. Solid State Mater. Sci.* **2018**, *22*, 243–254. [[CrossRef](#)]
5. Liu, D.; Tian, H. Microstructure, mechanical and elevated temperature tribological behaviors of the diamond/Cu composites prepared by spark plasma sintering method. *Diam. Relat. Mater.* **2019**, *91*, 138–143. [[CrossRef](#)]
6. Hayat, M.D.; Singh, H. Enhanced interfacial bonding in copper/diamond composites via deposition of nano-copper on diamond particles. *JOM* **2022**, *74*, 949–953. [[CrossRef](#)]
7. Wu, L.J.; Zhang, G. Study on microstructure and tribological performance of diamond/Cu composite coating via supersonic laser deposition. *Coatings* **2020**, *10*, 276. [[CrossRef](#)]
8. Hagio, T.; Park, J.H. Electrodeposition of nano-diamond/copper composite platings: Improved interfacial adhesion between diamond and copper via formation of silicon carbide on diamond surface. *Surf. Coat. Technol.* **2020**, *403*, 126322. [[CrossRef](#)]
9. Bai, G.; Li, N. High thermal conductivity of Cu-B/diamond composites prepared by gas pressure infiltration. *J. Alloys Compd.* **2018**, *735*, 1648–1653. [[CrossRef](#)]
10. Wang, L.H.; Li, J.W. Combining Cr pre-coating and Cr alloying to improve the thermal conductivity of diamond particles reinforced Cu matrix composites. *J. Alloys Compd.* **2018**, *749*, 1098–1105. [[CrossRef](#)]
11. Lei, L.; Bolzoni, L. High thermal conductivity and strong interface bonding of a hot-forged Cu/Ti-coated-diamond composite. *Carbon* **2020**, *168*, 553–563. [[CrossRef](#)]
12. Pan, Y.P.; He, X.B. Optimized thermal conductivity of diamond/Cu composite prepared with tungsten-copper-coated diamond particles by vacuum sintering technique. *Vacuum* **2018**, *153*, 74–81. [[CrossRef](#)]
13. Yang, L.; Sun, L. Thermal conductivity of Cu-Ti/diamond composites via spark plasma sintering. *Diam. Relat. Mater.* **2019**, *94*, 37–42. [[CrossRef](#)]
14. Luo, F.; Jiang, X.S. Microstructures, mechanical and thermal properties of diamonds and graphene hybrid reinforced laminated Cu matrix composites by vacuum hot pressing. *Vacuum* **2023**, *207*, 111610. [[CrossRef](#)]
15. Chen, H.; Jia, C. Interfacial characterization and thermal conductivity of diamond/Cu composites prepared by two HPHT techniques. *J. Mater. Sci.* **2011**, *47*, 3367–3375. [[CrossRef](#)]
16. Jia, J.H.; Bai, S.X. Effect of tungsten based coating characteristics on microstructure and thermal conductivity of diamond/Cu composites prepared by pressureless infiltration. *Ceram. Int.* **2019**, *45*, 10810–10818. [[CrossRef](#)]
17. Chen, C.; Guo, H. Thermal conductivity of diamond/copper composites with a bimodal distribution of diamond particle sizes prepared by pressure infiltration method. *Rare Met.* **2011**, *30*, 408–413. [[CrossRef](#)]

18. Li, J.W.; Zhang, H.L. Optimized thermal properties in diamond particles reinforced copper-titanium matrix composites produced by gas pressure infiltration. *Compos. Part A Appl. Sci. Manuf.* **2016**, *91*, 189–194. [[CrossRef](#)]
19. Gorunov, A.I. Features of coatings obtained by supersonic laser deposition. *J. Therm. Spray Technol.* **2018**, *27*, 1194–1203. [[CrossRef](#)]
20. Yin, S.; Hassani, M. Unravelling the deposition mechanism of brittle particles in metal matrix composites fabricated via cold spray additive manufacturing. *Scr. Mater.* **2021**, *194*, 113614. [[CrossRef](#)]
21. Lupoi, R.; Sparkes, M. High speed titanium coatings by supersonic laser deposition. *Mater. Lett.* **2011**, *65*, 3205–3207. [[CrossRef](#)]
22. Riveiro, A.; Lusquinos, F. Supersonic laser spray of aluminium alloy on a ceramic substrate. *Appl. Surf. Sci.* **2007**, *254*, 926–929. [[CrossRef](#)]
23. Li, B.; Jin, Y. Solid-state fabrication of WCp-reinforced Stellite-6 composite coatings with supersonic laser deposition. *Surf. Coat. Technol.* **2017**, *321*, 386–396. [[CrossRef](#)]
24. Tsukamoto, K.; Uchiyama, F. Ceramic coating technique using laser spray process. *Surf. Eng.* **2013**, *6*, 45–48. [[CrossRef](#)]
25. Li, N.; Wang, Q. Research progress of coating preparation on light alloys in aviation field: A review. *Materials* **2022**, *15*, 8535. [[CrossRef](#)]
26. Yin, S.; Cizek, J. Metallurgical bonding between metal matrix and core-shelled reinforcements in cold sprayed composite coating. *Scr. Mater.* **2020**, *177*, 49–53. [[CrossRef](#)]
27. Wei, C.; Xu, X. Titanium coating on the surface of diamond particles by a novel rapid low-temperature salt bath plating method. *Chem. Phys. Lett.* **2020**, *761*, 138091. [[CrossRef](#)]
28. Wu, Y.P.; Luo, J.B. Critical effect and enhanced thermal conductivity of Cu-diamond composites reinforced with various diamond prepared by composite electroplating. *Ceram. Int.* **2019**, *45*, 13225–13234. [[CrossRef](#)]
29. Wang, Y.; Deng, N. The effect of Fe/Al ratio and substrate hardness on microstructure and deposition behavior of cold-sprayed Fe/Al coatings. *Materials* **2023**, *16*, 878. [[CrossRef](#)]
30. Daodon, W.; Saetang, V. Improvement of frictional property of AISI D2 tool steel surface against JIS SPFC 980Y advanced high-strength steel by using laser texturing process. *Lubricants* **2023**, *11*, 68. [[CrossRef](#)]
31. Zhou, H.; Yao, P. Friction and wear maps of copper metal matrix composites with different iron volume content. *Tribol. Int.* **2019**, *132*, 199–210. [[CrossRef](#)]
32. Liu, S.; Yu, X. Effect of Cu-doped carbon quantum dot dispersion liquid on the lubrication performance of polyethylene glycol. *Lubricants* **2023**, *11*, 86. [[CrossRef](#)]

Disclaimer/Publisher’s Note: The statements, opinions and data contained in all publications are solely those of the individual author(s) and contributor(s) and not of MDPI and/or the editor(s). MDPI and/or the editor(s) disclaim responsibility for any injury to people or property resulting from any ideas, methods, instructions or products referred to in the content.